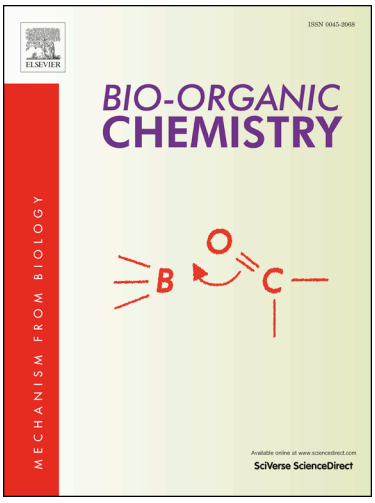

EGFR inhibitors and apoptotic inducers: Design, synthesis, anticancer activity and docking studies of novel xanthine derivatives carrying chalcone moiety as hybrid molecules

Hesham A. Abou-Zied, Bahaa G.M. Youssif, Mamdouh F.A. Mohamed, Alaa M. Hayallah, Mohamed Abdel-Aziz

PII: S0045-2068(18)31402-0
DOI: https://doi.org/10.1016/j.bioorg.2019.102997
Article Number: 102997
Reference: YBIOO 102997

To appear in: *Bioorganic Chemistry*

Received Date: 1 December 2018
Revised Date: 21 March 2019
Accepted Date: 17 May 2019

Please cite this article as: H.A. Abou-Zied, B.G.M. Youssif, M.F.A. Mohamed, A.M. Hayallah, M. Abdel-Aziz, EGFR inhibitors and apoptotic inducers: Design, synthesis, anticancer activity and docking studies of novel xanthine derivatives carrying chalcone moiety as hybrid molecules, *Bioorganic Chemistry* (2019), doi: https://doi.org/10.1016/j.bioorg.2019.102997

EGFR inhibitors and apoptotic inducers: Design, synthesis, anticancer activity and docking studies of novel xanthine derivatives carrying chalcone moiety as hybrid molecules

Hesham A. Abou-Zied[1], Bahaa G.M. Youssif[2,3]*, Mamdouh F. A. Mohamed[4], Alaa M. Hayallah[1,2]*, Mohamed Abdel-Aziz[5]

Pharmaceutical Organic Chemistry Department, Faculty of Pharmacy, Deraya University, Minia, Egypt; [2]Pharmaceutical Organic Chemistry Department, Faculty of Pharmacy, Assiut University, Assiut 71526, Egypt; [3]Department of Pharmaceutical Chemistry, College of Pharmacy, Jouf University, Aljouf, Sakaka 2014, Saudi Arabia; [4]Department of Pharmaceutical Chemistry, Faculty of Pharmacy, Sohag University, 82524 Sohag, Egypt; [5]Department of Medicinal Chemistry, Faculty of Pharmacy, Minia University, 61519-Minia, Egypt.

Short running title: Synthesis, anticancer, and docking study of new xanthine-chalcone hybrids

**To whom correspondence should be addressed:*

Bahaa G. M. Youssif. **Ph.D**. Pharmaceutical Organic Chemistry Department, Faculty of Pharmacy, Assiut University, Assiut 71526, Egypt

Tel.: (00966)-537240294

E-mail address: bgyoussif@ju.edu.sa

Alaa M. Hayallah. Ph.D. Pharmaceutical Organic Chemistry Department, Faculty of Pharmacy, Deraya University, Minia, Egypt

Tel.: (002)-01283410110

E-mail address: alaa_hayalah@yahoo.com

Abstract

One of the helpful ways to improve the effectiveness of anticancer agents and weaken drug resistance is to use hybrid molecules. therefore, the current study intended to introduce **20** novel xanthine/chalcone hybrids **9-28** of promising anticancer activity. Compounds **10**, **11**, **13**, **14**, **16**, **20** and **23** exhibited potent inhibition of cancer cells growth with IC_{50} ranging from 1.0±0.1 to 3.5±0.4 μM compared to doxorubicin with IC_{50} ranging from 0.90± 0.62 to 1.41 ± 0.58 μM and that compounds **11** and **16** were the best. To verify the mechanism of their anticancer activity, compounds **10**, **11**, **13**, **14**, **16**, **20** and **23** were evaluated for their EGFR inhibitory effect. The study results revealed that compound **11** showed IC_{50} = 0.3 μM on the target enzyme which is more potent than staurosporine reference drug (IC_{50} = 0.4 μM). Accordingly, the apoptotic effect of the most potent compounds **11** was extensively investigated and showed a marked increase in Bax level up to 29 folds, and down-regulation in Bcl2 to 0.28 fold, in comparison to the control. Furthermore, the effect of compound **11** on Caspases 3 and 8 was evaluated and was found to increase their levels by 8 and 14 folds, respectively. Also, the effect of compound **11** on the cell cycle and its cytotoxic effect were examined. Moreover, a molecular docking study was adopted to confirm mechanism of action.

Keywords: Xanthine; Chalcone; Hybrids; EGFR; Anti-proliferative; Apoptotic assay.

Graphical abstract

EGFR inhibitors and apoptotic inducers: Design, synthesis, anticancer activity and docking studies of novel xanthine derivatives carrying chalcone moiety as hybrid molecules

Hesham A. Abou-Zied1, Bahaa G.M. Youssif2,3, Mamdouh F. A. Mohamed4, Alaa M. Hayallah1,2*, Mohamed Abdel-Aziz5

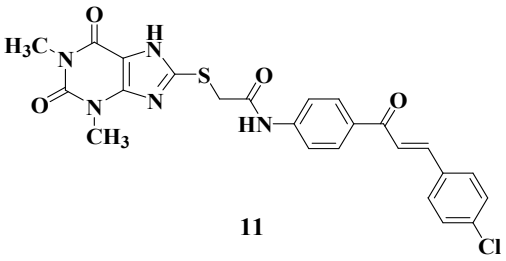

11

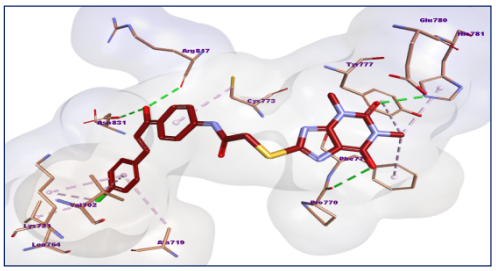

MCF-7	1.3±0.9 µM
EGFR	0.3 µM
Caspase-3	532.2 ±5.13 Pg/ml
Caspase-8	1.21 ng/ml
Bax	Up to 29 folds
Bcl-2	3.48 fold change

Highlights

- A series of **20** novel compounds contain xanthine-chalcone hybrid was designed and synthesized.
- The synthesized hybrids were evaluated for their *in vitro* antiproliferative activity against different human cancer cell lines.
- Compounds **10**, **11**, **13**, **14**, **16**, **20** and **23** exhibited potent inhibition of cancer cells.
- Compound **11** was selected for cell cycle analysis and apoptosis assay
- Results revealed that these compounds showed programmed cell death and cell cycle arrest
- Molecular modeling for compounds **10**, **11**, **20** and **21** were done against 3D crystal structures of EGFR.

1. INTRODUCTION

Cancer is one of the primary causes of death universal [1]. Most patients who have been diagnosed with cancer suffer from poor quality of life due to adverse proceedings associated with cancer [2]. One of the most effective methods of suppressing tumor growth and tumor eradication is chemotherapy [3]. However, many patients undergoing chemotherapy have associated side effects such as thrombocytopenia, anemia, nausea and vomiting [4]. Although, many research studies have reported potential chemotherapeutic effects of new compounds, research is still underway in the hope of finding new anticancer agents with improved efficacy and high degree of safety toward normal host cells [5, 6]. Methylxanthine derivatives such as caffeine **(1)** and theophylline **(2)** were found to induce apoptosis, and promote cytotoxicity induced by doxorubicin [7]. Theophylline was found to induce programmed cell death in various human cancer cell line and in a malignantly transformed granulosa cell line when synergizing with gemcitabine or cisplatin [8]. The mechanism of the apoptogenic effect of theophylline has been found to involve reduction of intracellular levels of the antiapoptotic mediator Bcl2. Therefore, theophylline-based moieties comprise an attractive scaffold for structural modification in search of novel antiproliferative agents with diverse pharmacodynamics [9]. Besides theophylline and its congeners other methylxanthines have been also evaluated for anticancer and chemosensitivity-modulating agents. Pentoxifylline **(3)** was found to increase the effectiveness of both radiotherapy and chemotherapy [10, 11]. A combination schedule of pentoxifylline with doxorubicin, exhibited synergistic action and inhibited cell proliferation to a superior extent with regard to each drug used alone [12].

Recent studies demonstrated that molecular hybridization of chalcone units with biologically active pharmacophore produced new hybrids with synergistic biological activity [13]. For example, Compound **4** showed remarkable cytotoxic activity against human lung adenocarcinoma A549 cells with IC_{50} of 4.4 μM compared to cisplatin. The further mechanistic study of compound **4** demonstrated that 1, 2, 4-triazole-chalcone hybrids induced apoptosis via increased level of proapoptotic protein Bax, release of Cytochrome C from mitochondria and activation of caspase-3/8/9 proteins [13]. The presence of chalcone derivativesas a key element, or a substituent or as a side-chain in different biologically active compounds has encouraged the synthetic chemists to synthesize new compounds bearing this moiety and hence, different newly synthesized chalcones with their anti-cancer activities are discussed [14-17].

Encouraged by all these facts, the present work aimed at gathering two bioactive entities chalcone and xanthine derivative in only one compact hybrid structure for the purpose of synergism and/or decreasing the expected adverse effects. Synthesis of novel hybrid compounds based on xanthine and chalcone pharmacophores through S-alkylation of 1,3,8-trisubstituted and 1,8-disubstituted xanthine derivatives with different acetylated chalcones.

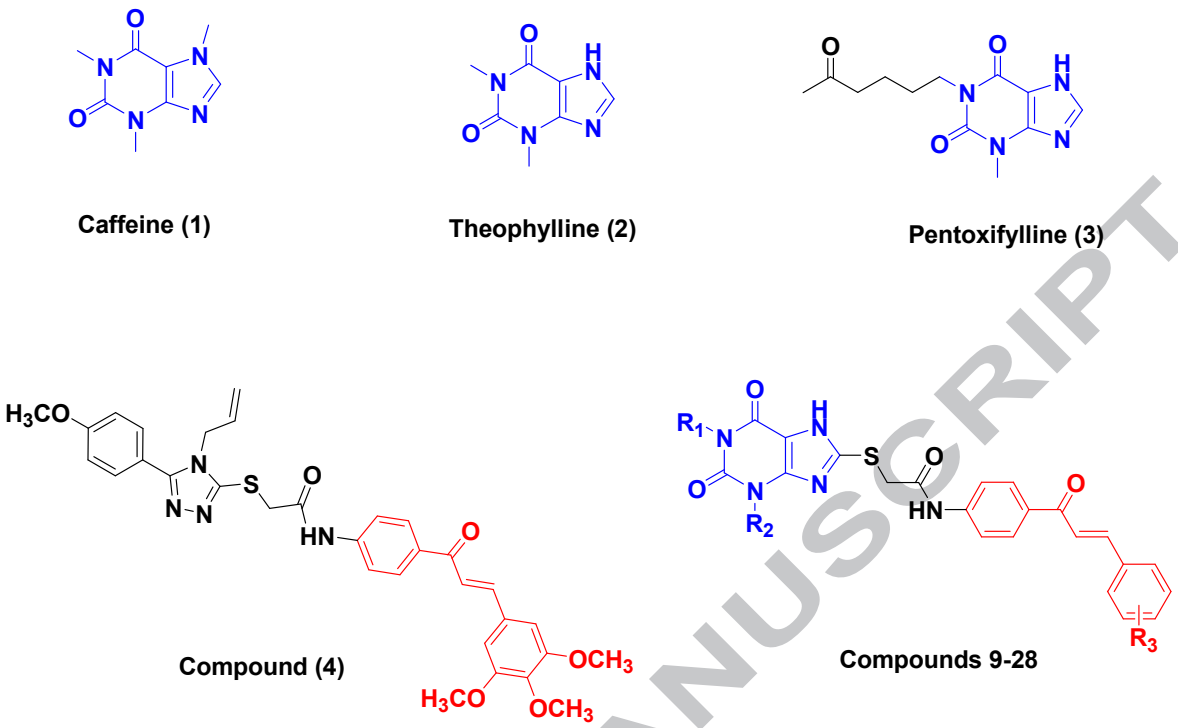

Figure 1: Structure of compounds **1-4** and rational compounds **9-28**.

the newly synthesized compounds were identified using different spectroscopic techniques including: IR, ^{1}H NMR, ^{13}C NMR as well as elemental microanalysis. All target compounds were evaluated for their anti-proliferative activity *in vitro* on selected human cancer cell lines. In order to investigate the mechanistic pathways of the anticancer activity of the target compounds, the most potent hybrids were selected to perform further investigations such as EGFR assay, cell cycle analysis, and apoptosis markers.

2. RESULTS AND DISCUSSION

2.1. Chemistry

The synthesis of purine-2,6-diones **4a-b** was described in **Scheme 1**. The intermediate 6-Amino-1,3-dimethyluracil **1a** was prepared by condensation of *N,N'*-dimethylurea with cyanoacetic acid, followed by stirring in 70% (w/v) sodium hydroxide solution to afford the desired compound **1a** [18-20]. 6-Amino-3-methyluracil **1b** was prepared by refluxing 6-aminouracil in hexamethyldisilazane (HMDS) in presence of a catalytic amount of ammonium sulfate, followed by addition of methyl iodide to afford the desired N3-substituted 6-aminouracil [21, 22]. Nitrosation of compounds **1a-b** using sodium nitrite in 50% aqueous acetic acid yielded **2a-b**. Sodium dithionite reduction of **2a-b** in aqueous ammonia solution yielded compounds **3a-b**. Direct cyclization of 5,6-diamino-1,3-dimethyluracil **3a** using carbon disulfide in DMF under reflux for 5 h afforded compound **4a** while, Compound **4b** was prepared by direct cyclization of 5,6-diamino-1,3-dimethyluracil **3b** using carbon disulfide in ethanolic solution of KOH under reflux for 4 h.

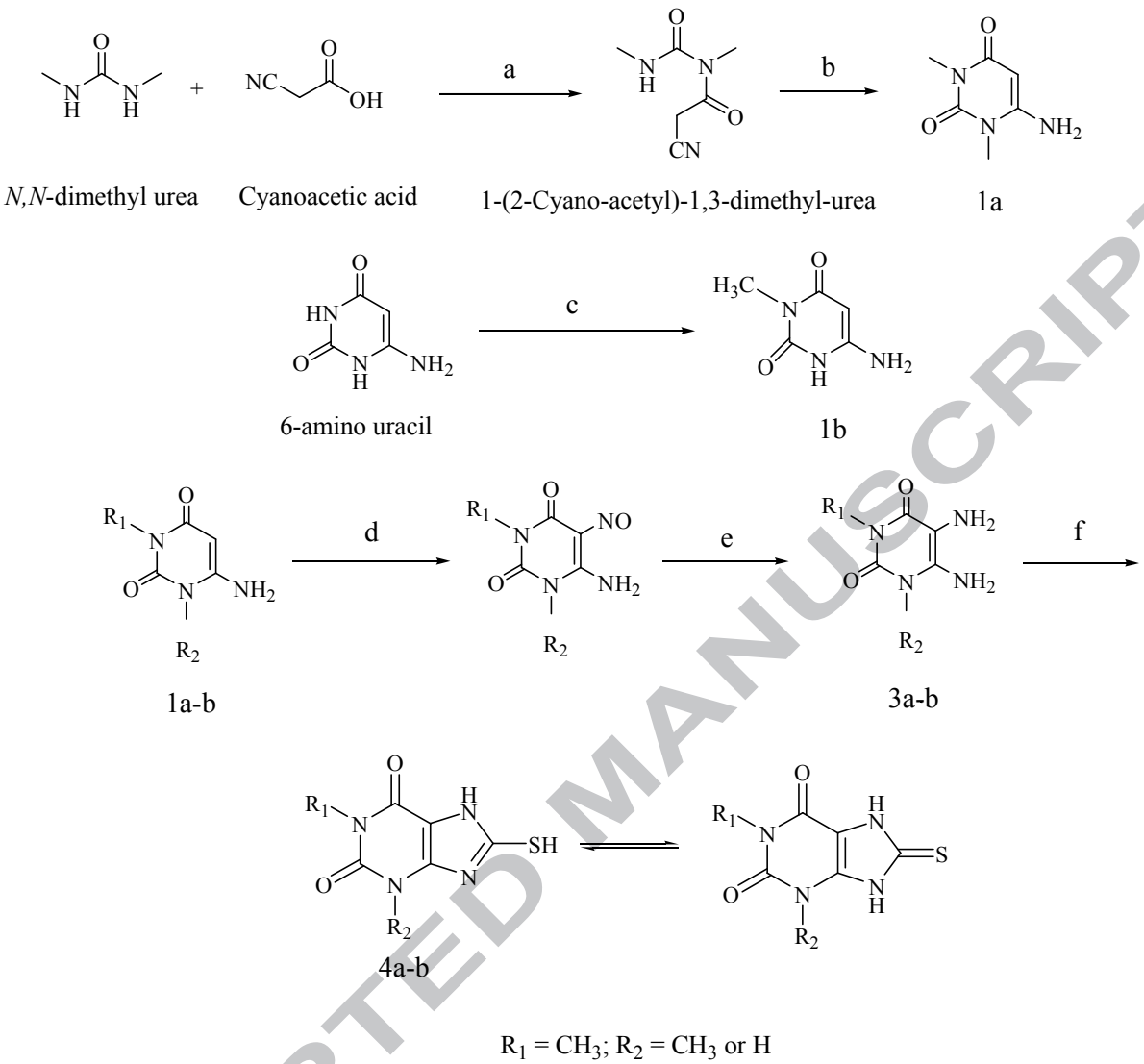

Scheme 1: Synthesis of Xanthine derivatives **4a-b**.

Reagents and reaction condition: a) acetic anhydride; b) NaOH 70 %; c) 1. HMDS, 2. CH_3I, 3. $Na_2S_2O_3$, $NaHCO_3$; d) $NaNO_2/CH_3COOH$; e) 12.5% aq. NH_3/ $Na_2S_2O_4$; f) CS_2/ (DMF or ethanol)/ reflux.

The target hybrid molecules **9-28** were prepared according to **Scheme 2**. Chalcone derivatives **7a-j** were synthesized by a base catalyzed Claisen–Schmidt condensation of 4-aminoacetophenone with substituted benzaldehyde derivatives [23]. Stirring chalcones **7a-j** with bromoacetylbromide in biphasic layer from potassium carbonate solution in dichloromethane forming the corresponding acetylated chalcones **8a-j**. Alkylation of compounds **4a-b** with acylated chalcones **8a-j** afford the target

compounds **9-28** in good yields. The chemical structures of **9-28** were elucidated by ^{1}H NMR and ^{13}C NMR spectroscopy. The **^{1}H NMR** spectrum of compound **11** as a representative example of 1,3-dimethyl xanthine derivatives **9-18** revealed the appearance of asinglet signal with three protons integration at δ 3.22 ppm represented (N1-C*H*$_3$), while (N3-C*H*$_3$) appeared at δ 3.39 ppm as singlet signal with three protons integration, appearance of a singlet signal with two protons integration at δ 4.26 ppm assigned for methylene protons (S-C*H*$_2$-CO) of the linker. Furthermore, the two chalcone protons appears at aromatic region as doublet signal at δ 7.73 and δ7.93 ppm with coupling constant *J* = 15.00 Hz, two doublet of doublet signals related to aromatic protons and also, appearance of a singlet signal at 10.71 ppm assigned to amide proton N*H*, characteristic broad singlet signal at δ13.63 ppm represents (N7-*H*) of xanthine nucleus. The **^{13}C NMR** spectrum of **11** showed the appearance of two peaks at δ 28.18 and δ 30.20 ppm assigned to N1-CH_3 and N3-CH_3 of xanthine moiety, while methylene carbon of the linker peak at δ 37.09 ppm, all other carbons appear at their expected chemical shifts. **^{1}H NMR** spectrum of compound **19** as a representative example of 3-methyl xanthine derivatives **19-28** showed asinglet signal at δ 3.18 ppm represented (N1-C*H*$_3$), a singlet signal at δ 4.24 ppm of methylene protons (S-C*H*$_2$-CO) of the linker. Moreover, the two chalcone protons appears at aromatic region as doublet signal at δ 7.75 and δ 7.97 ppm with coupling constant *J* = 15.08 Hz and also, appearance of a broad singlet signal at δ11.89 ppm represents (N1-*H*) of xanthine nucleus. The **^{13}C NMR** spectrum of **19** showed the appearance of one peak at δ 27.43 ppm related to N1-CH_3 of xanthine moiety, while methylene carbon of the linker peak at δ36.96 ppm.

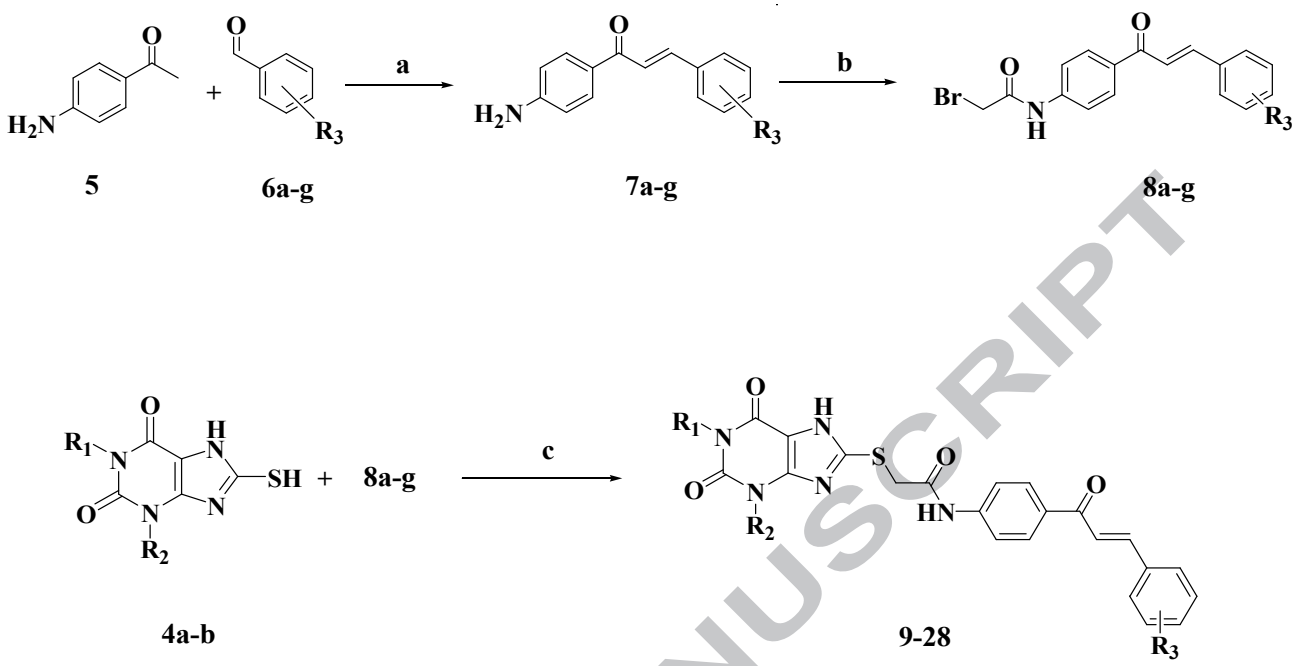

5 6a-g 7a-g 8a-g

4a-b 9-28

Comp	R_1	R_2	R_3	Comp	R_1	R_2	R_3
9	Methyl	Methyl	H	**19**	Methyl	H	H
10	Methyl	Methyl	2-Cl	**20**	Methyl	H	2-Cl
11	Methyl	Methyl	4-Cl	**21**	Methyl	H	4-Cl
12	Methyl	Methyl	4-Br	**22**	Methyl	H	4-Br
13	Methyl	Methyl	4-OCH_3	**23**	Methyl	H	4-OCH_3
14	Methyl	Methyl	3,4-di-OCH_3	**24**	Methyl	H	3,4-di-OCH_3
15	Methyl	Methyl	3,4,5-tri-OCH_3	**25**	Methyl	H	3,4,5-tri-OCH_3
16	Methyl	Methyl	3-NO_2	**26**	Methyl	H	3-NO_2
17	Methyl	Methyl	4-CH_3	**27**	Methyl	H	4-CH_3
18	Methyl	Methyl	2,4-di-CH_3	**28**	Methyl	H	2,4-di-CH_3

Scheme 2: Synthesis of target compounds **9-28**.

Reagents and reaction conditions: a) NaOH 60%; b) $BrCH_2COBr$/ CH_2Cl_2; c) TEA/ acetonitrile

2.2. Evaluation of biological Activity

2.2.1. *In vitro* anticancer activity

2.2.1.1. Cell viability assay

Cell viability assay was carried out using human mammary gland epithelial cell line (MCF-10A). All synthesized compounds **9-28** were treated with MCF-10A cells for 4 days and 3-(4,5-dimethylthiazol-2-yl)-2,5-diphenyltetrazolium bromide (MTT) assay was used to determine the viability of cells. All compounds were exhibited non-toxic with the majority of them reveling more than 90% cell viability at the concentration of 50 μM.

2.2.1.2. Antiproliferative activity

All final hybrids **9-28** were evaluated for their antiproliferative activity against four cancer cell lines, human pancreas cancer cell line (Panc-1), breast cancer cell line (MCF-7), colon cancer cell line (HT-29) and epithelial cancer cell line (A-549), using MTT assay and Doxorubicin was used as the reference compound. GraphPad Prism software (GraphPad Software, San Diego, CA, USA) was used to calculate the median inhibition concentration (IC_{50}) for all compounds.

As shown in **Table 1**, seven most active compounds **10**, **11**, **13**, **14**, **16**, **20** and **23** among both 1,3-dimethyl substituted xanthine and 1-methyl substituted xanthine derivatives exhibited potent inhibition of cancer cells growth with IC_{50} ranging from 1.0±0.1 to 3.5±0.4 μM compared to doxorubicin with IC_{50} ranging from 0.90± 0.62 to 1.41 ± 0.58 μM. Compound **16** possessed highest anti cancer activity among all new hybrids against cancer cell growth with IC_{50}1.0±0.1 μM for the MCF-7 breast cancer cell line. All other compounds showed moderate activity against growth of cancer cell lines. Compound **16** displayed the peak anticancer potential and it was bearing 1,3-

dimethyl xanthine backbone while on the other side compound **26** was bearing same substitution pattern as compared to **16** and difference was 1-methyl xanthine moiety but it showed almost six folds less activity. Compound **11** of 1,3-dimethyl xanthine (R_3 = 4-Cl) class showed highly potent anticancer activity (IC_{50} = 1.3μM) against breast cancer cell line (MCF-7). Interestingly, compound **21**, with R_3 = 4-Cl at position of 1-methyl xanthine core showed weak cytotoxicity against breast cancer cell line (IC_{50} = 9.4μM), which is 7 fold less activity than **11**. From the above-mentioned results, it can be concluded that most of 1,3-dimethyl xanthine hybrids **9-18** were better antiproliferative agents of cancer cells as compared to other derivatives **19-28** bearing 1-methyl xanthine core.

Table 1: Antiproliferative activity of the target compounds **9-28**.

Compound number	**Antiproliferative activity IC50 ± SEM (μM)**			
	Panc-1	**MCF-7**	**HT-29**	**A-549**
9	4.9±2.4	5.1±2.4	5.9±1.7	6.7±1.5
10	1.9±1.1	1.8±0.7	2.3±1.6	1.7±0.7
11	1.7±1.6	1.3±0.9	1.7±0.9	1.8±0.7
12	2.91±0.2	2.8±0.5	3.7±0.4	3.5±0.2
13	2.1±1.1	1.1±0.7	1.9±1.6	2.2±0.7
14	2..61±0.2	1.5±0.5	3.4±0.4	3.2±0.2
15	3.3±2.4	4.5±2.4	4.3±1.7	5.1±1.5
16	1.3±0.9	1.0±0.1	1.2±0.7	1.5±0.5
17	9.7±2.1	11.1±1.7	11.6±1.5	10.2±1.9
18	5.6±2.4	6.4±2.4	6.1±1.7	7.1±1.5
19	6.9±1.5	6.8±2.7	6.2±2.4	7.7±1.6

20	3.3±0.9	3.0±0.1	3.2±0.7	3.5±0.5
21	7.8±1.7	9.4±2.1	6.5±2.4	7.3±2.1
22	7.8±1.7	9.4±2.1	6.5±2.4	7.3±2.1
23	2.7±1.6	2.3±0.9	2.7±0.9	2.8±0.7
24	6.2±1.5	7.4±1.4	8.9±2.7	7.4±2.1
25	4.6±1.2	5.3±1.2	3.1±1.4	6.6±1.6
26	6.2±1.5	6.4±2.7	5.3±2.4	6.7±1.6
27	5.5±2.5	5.9±3.0	6.7±2.4	6.1±1.1
28	6.8±1.5	7.2±1.7	8.2±1.5	8.1±2.1
Doxorubicin	1.41 ± 0.58	0.90± 0.62	1.01 ± 0.82	1.21 ± 0.80

Moreover, the substitution variations (R_3) at position 4 of chalcone phenyl ring can be correlated with the activity of compounds. Interestingly, in 1,3-dimethyl xanthine series three compounds **10**, **11** and **16** with an electron withdrawing substitution groups on chalcone phenyl ring showed better inhibitory activity against almost all the cell lines tested compared to compounds **17** and **18** which were bearing electron donating substitution groups and that NO_2, Cl and OMe were the best.

2.2.2. Inhibition of Epidermal Growth Factor Receptor Activity (EGFR-TK)

EGFR-TK assay was performed to assess the EGFR inhibitory potency of novel compounds and the results are included in **Table 2**. The results from this assay complement the findings of cancer cell-based assay. All investigated compounds **10**, **11**, **13**, **14**, **16** and **23** exhibited inhibition of EGFR with IC_{50} ranging from 0.3 to 1.6 μM. According to data presented, three derivatives **10**, **11** and **14** selected from xanthine-chalcone hybrids were found to be most potent and their EGFR inhibitory activities were close to the positive reference staurosporine (IC_{50} = 0.4 μM). This

experiment shows that these compounds are potent EGFR inhibitors and can possibly be used as anticancer agents.

Table 2: Effects of compounds **10**, **11**, **13**, **14**, **16**, **23**, and **staurosporine** on EGFR.

Compd. No.	EGFRIC_{50}(μM)
10	**0.6**
11	**0.3**
13	**1.5**
14	**0.9**
16	**1.6**
23	**1.2**
staurosporine	**0.4**

2.2.3. Apoptotic markers activation assay

Apoptosis, also called programmed cell death, involves several morphological and biochemical events [24]. There are proapoptotic proteins such as Bad, Bax, Bid, BcL-Xs and Bim, as well as antiapoptotic members such as Bcl-2, Bc-LXl and Bcl-W [25]. Anti-apoptotic proteins act as inhibitors of apoptosis by blocking the release of cytochrome-c while proapoptotic members function as activators of its release. When the ratio of proapoptotic proteins exceeds antiapoptotic ones, the outer mitochondrial membrane becomes permeable leading to a cascade of events. Cytochrome C is released which activates caspase-9 which then activates caspase-3 which in turn stimulates apoptosis by attacking many valuable proteins required by the cell [26].

2.2.3.1. Caspase-3 activation assay

Xanthine-chalcone hybrids **10, 11, 13, 14, 16** and **23** were evaluated as caspase-3 activators against Panc-1 human pancreas cancer cell line and the results are listed in **Table 3**. The results revealed that compounds **11**, **14** and **23** possessed remarkable over expression of caspase-3 protein level (532.2 ±5.13, 373.2 ±3.92 and 387.4 ±12.2 pg/mL, respectively) compared to the reference staurosporine (503.2 ± 4.22 pg/mL). The most active compound which was bearing 4-Cl on the phenyl ring of chalcone moiety **11** caused over-expression of caspase-3 protein level (532.2 ±5.13 pg/mL) in Panc-1human pancreas cancer cell line about **8 folds** higher than control, and higher than that of staurosporine **(Figure 2)**. So, the above results may be considered as a suggestion that apoptosis may be attributed to over-expression of caspase-3 which induced by the tested compounds.

Table 3: Caspase-3 level for compounds **10**, **11**, **13**, **14**, **16**, **23**, and staurosporine in human pancreas cancer cell line (Panc-1).

Compound Number	**Caspase-3**	
	Conc (Pg/ml)	Fold change
10	315.20 ± 9.27	4.80
11	532.20 ± 5.13	8.10
13	254.70 ± 3.14	3.87
14	373.20 ± 3.92	5.68
16	339.80 ± 2.19	5.17
23	387.40 ± 12.2	5.90
Staurosporine	503.20 ± 4.22	7.66
Control	65.64	1

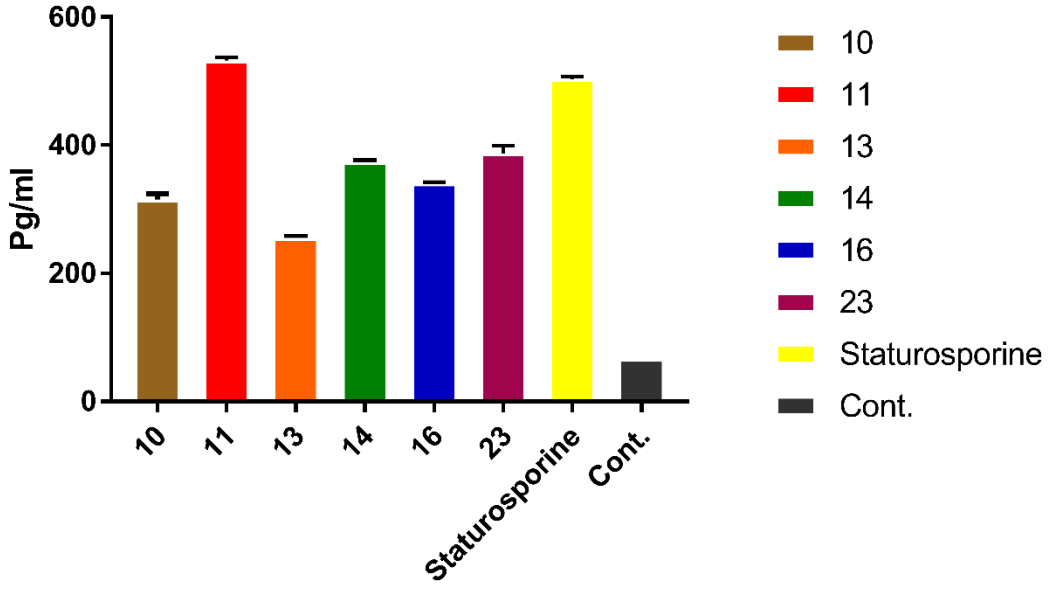

Figure 2: Caspase-3 level for compounds **10**, **11**, **13**, **14**, **16**, **23**, and **staurosporine** in human pancreas cancer cell line (Panc-1).

2.2.3.2. Caspase-8, Bax and Bcl-2 levels assay

The most three active caspase-3 activator xanthine-chalcone hybrids **11**, **14** and **16** were further studied for their effect on caspase-8, Bax and Bacl-2 levels against Panc-1human pancreas cancer cell line using staurosporine as a reference, which are mentioned in **Table 4**. The results showed that all of the tested compounds revealed remarkable increase in both caspase-8 and Bax levels compared to staurosporine. compound **14** which was bearing 3,4-dimethoxy groups on the phenyl ring of chalcone moiety possessed the maximum over-expression of caspapse-8 level (1.43 ng/mL) followed by compound **11** (1.21 ng/mL) and that of the reference doxorubicin (1.755 ng/mL) **(Figure 3)**. Moreover, 1,3-dimethyl xanthine-chalcone hybrid **11** showed a comparable induction of Bax (235 pg/mL) compared to doxorubicin (276 pg/mL) with 25 fold higher than control untreated Panc-1 cancer cells. Finally, compound **16** which was bearing 3-NO_2 group on the phenyl ring of chalcone moiety

caused equipotent down-regulation of Bcl-2 protein level (1.22 ng/mL) followed by compound **11** (1.46 ng/mL) in Panc-1cell line compared to staurosporine (0.98 ng/mL).

Table 4: Caspase-8, Bax and Bcl-2 levels for compounds **11**, **14**, **16**, and **staurosporine** on human pancreas cancer cells (Panc-1).

Compound Number	Caspase-8		Bax		Bcl-2	
	Conc (ng/ml)	Fold change	Conc (Pg/ml)	Fold change	Conc (ng/ml)	Fold change
11	1.21	14.33	235.20	28.46	1.46	3.48
14	1.43	16.92	208.90	25.27	1.87	2.71
16	1.08	12.77	188.50	22.80	1.22	4.16
staurosporine	1.75	20.76	276.19	33.42	0.98	5.18
Control	0.084	1	8.26	1	5.08	1

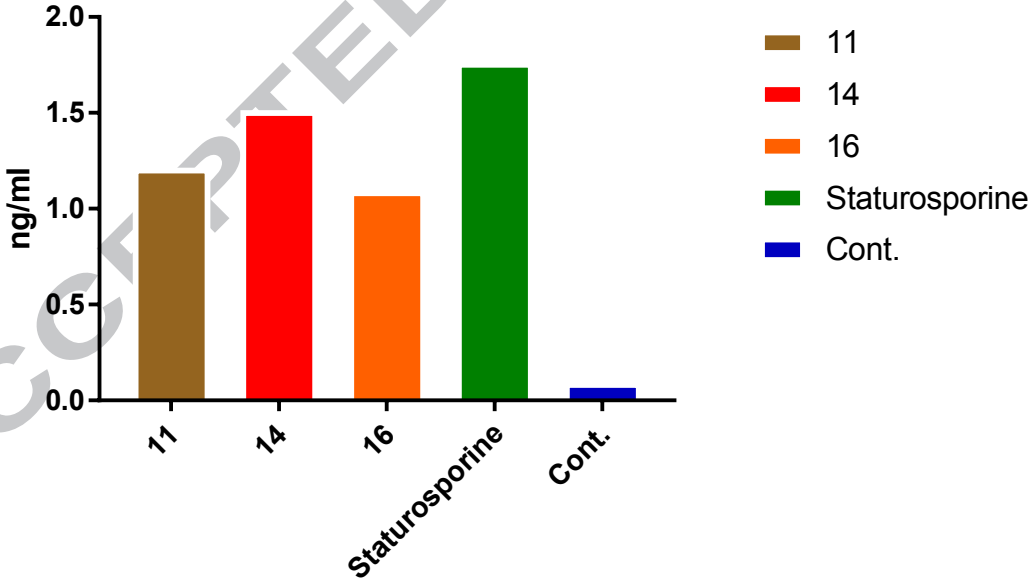

Figure 3 : Caspase-8 level for compounds **11**, **14**, **16**, and staurosporine in human pancreas cancer cells (Panc-1).

2.2.4. Flow cytometric Cell cycle analysis

Cell cycle analysis was performed for the most active compound **11** as standard drug against Panc-1 human pancreas cancer cell line.the percentages of cells of Panc-1cell in G0/G1 phase of the cell cycle in the control was 53.64% which recorded a noteworthy decrease to 26.67% upon treatment with compound **11** (**Figure 4** and **5**). These percentages were markedly increased at the G2/M phase to 48.56% for compound **11** due to accumulation of cells at this phase. Furthermore, it is obvious that the apoptotic cell percentage was increased from 1.79% for control untreated Panc-1cancer cell to 27.15% and 33.57% in treated cells with compound **11** and doxorubicin, respectively, (**Figure 5** and **6**). The results indicated that the percentage of the late apoptosis is more than that of early apoptosis which a good evidence for irreversible apoptosis caused by compounds **11** (**Figure 5** and **6**). According to the above results, it is clear that the compound **11** exhibited pre G1 apoptosis and cell cycle arrest at G2/M phase. Moreover, it is obvious that the tested compounds not cytotoxic but antiproliferative causing programmed cell death and cell cycle arrest.

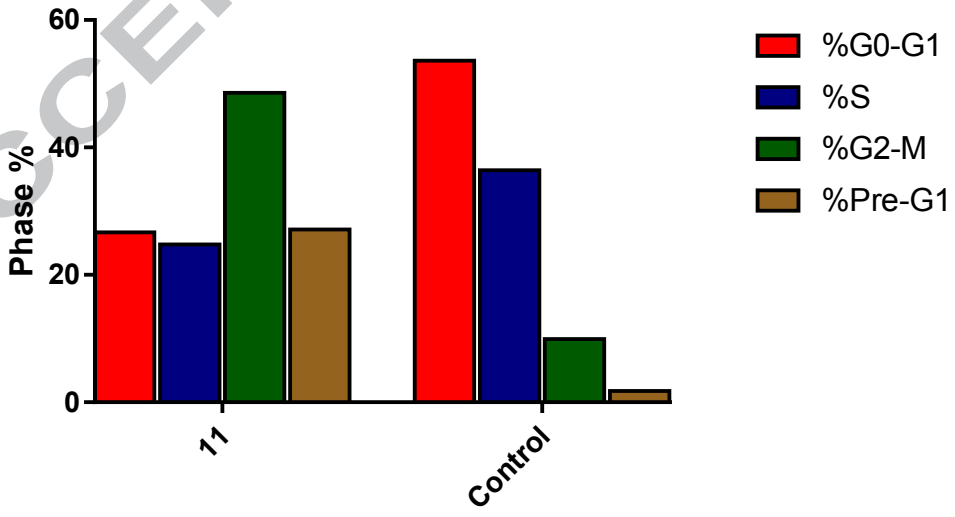

Figure 4: Cell cycle analysis on Panc-1cell line treated with compound **11**

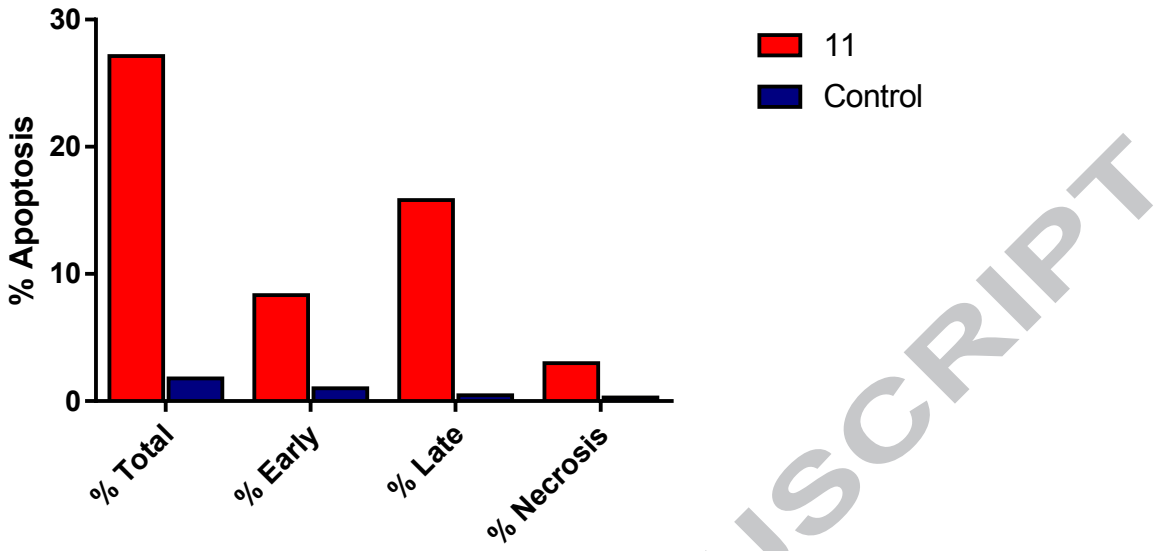

Figure 5: Percentage of apoptosis and necrosis for compound **11** onPanc-1cell line.

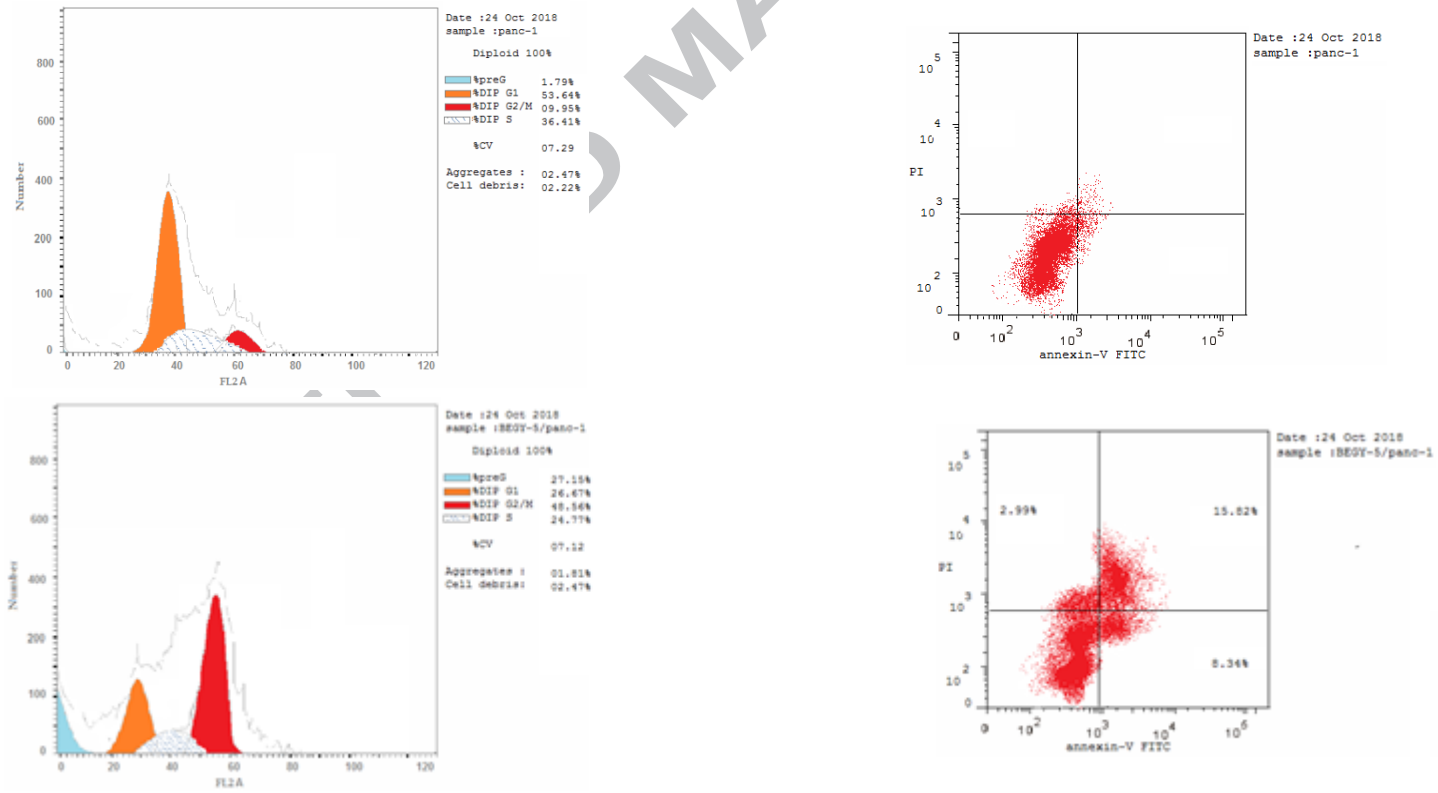

Figure 6: Cell cycle analysis and Apoptosis induction analysis using Annexin V/PI of compound **11** and control untreated RPMI8226 cell.

2.3. Docking study

In order to achieve some structural insights into EGFR inhibitory activities of the newly synthesized target compounds, a molecular docking simulation was done using CDOCKER embedded in the Discovery Studio software (Accelrys® software corporation, San Diego, USA). The 3D crystal structure of EGFR (PDB ID: 1M17) in complex with AQ4999 was used for this docking study [27, 28]. The most active disubstituted compounds **10** and **11** and their corresponding monosubstituted derivatives **20** and **21** were selected to be docked into EGFR binding site. The superimposition of the active docked poses inside protein binding pocket were shown in **Figure 7**. As a first step, validation of the docking protocol settings was done through the re-docking of the extracted co-crystallized ligand AQ4999 from the 3D structure 1M17 using the same protocol for the docked compounds. The used docking protocol closely reproduced the bound structure with RMSD value of 0.73 Å confirming the confidence in our docking study. Interestingly, the docking studies were in consistence with the results of EGFR inhibitory assay. The inspection of docking results revealed that the two docked ligands **10** and **11** adopted a nearly similar disposition inside the ATP binding pocket of the EGFR. The docking results of the most potent compound **10** and **11** against EGFR indicated that it fits well inside the ATP-active site. Also, it was found that chalcone moiety aligns near the DFG motif which plays a pivotal role in the kinase activity regulation forming a network of hydrogen bonds with Gly767, Met769 residues in compound **10** and with Arg817 and Asp831 residues in compound **11**, in addition to many hydrophobic interactions as shown in **Figure 8**. The xanthine moiety was oriented towards the hinge region and interestingly making two additional hydrogen bonds with Pro770 and His871 residue in both compounds, in addition to many hydrophobic interactions with Phe771 and

Tyr77, all these interactions may greatly contribute to the high in potency of compounds **10** and **11**.

On the hand, the docking results of the monosubstituted derivatives **20** and **21** against EGFR indicated that they adopted a similar binding pattern to that of compound **10** and **11**, however, there was adecrease in the number of engaged hydrogen bonds. Compound **20** forms one hydrogen bond with His781 residue, while compound **21** forms two hydrogen bonds with Met769 and his781 residue **Figure 9**. These results confirm our rationalized design that the disubstituted derivatives are more potent than the mono substituted ones.

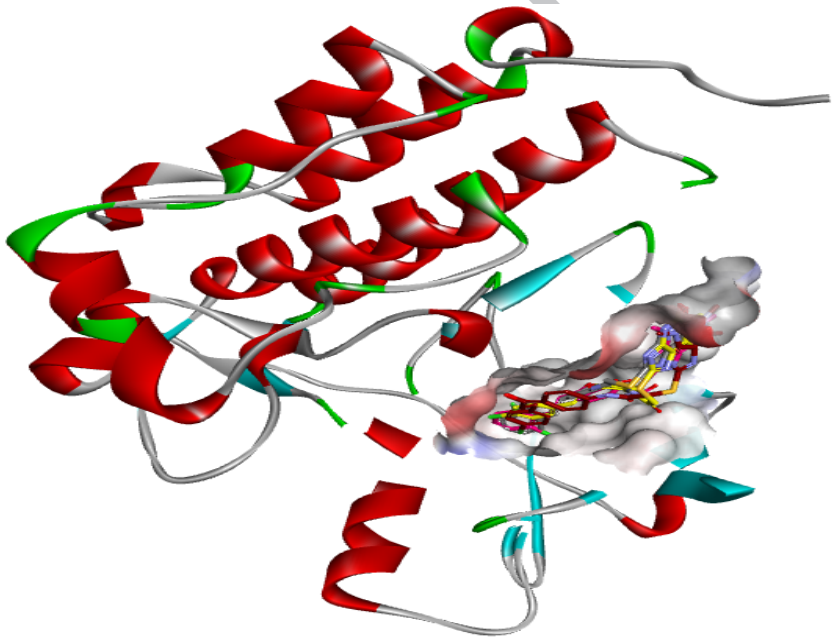

Figure 7: Superimposition of the active docked poses **10**, **11**, **20** and **21** inside the EGFR active site (PDB code: 1M17) where EGFR protein is represented as a secondary structure (flatribbon display style). The binding pockets are depicted according to atom charges. (For interpretation of the references to color in this figure legend, the reader is referred to the web version of this article.)

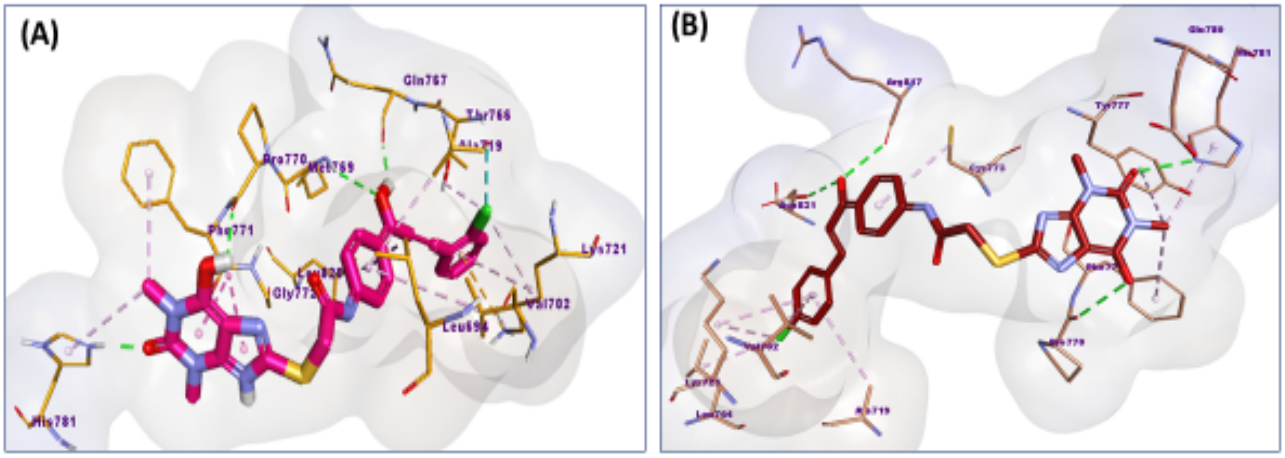

Figure 8: (**A**) Docking and binding pattern of compound **10** (pink) into ATP-active site of EGFR kinase (PDB code: 1M17); (**B**) Docking and binding pattern of compound **11** (red) into ATP-active site of EGFR kinase. Hydrogen bonds were represented as dashed green lines. All hydrogens were removed for the purposes of clarity.

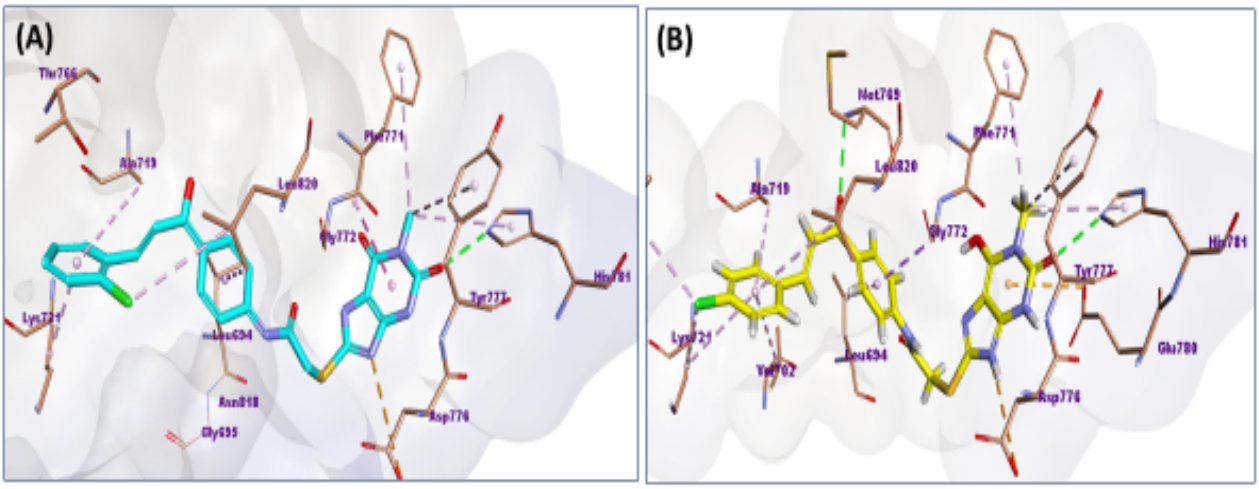

Figure 9: (**A**) Docking and binding pattern of compound **20** (cyan) into ATP-active site of EGFR kinase (PDB code: 1M17); (**B**) Docking and binding pattern of compound **21** (yellow) into ATP-active site of EGFR kinase. Hydrogen bonds were represented as dashed green lines.

4. EXPERIMENTAL

4.1. Chemistry

All reagents for synthesis were purchased from Sigma-Aldrich (St. Louis Mo., USA) and MERCK (Schuchardt, Germany). All solvents used in this work weren't further distilled before to be used. The Reactions were monitored by TLC (Thin-layer Chromatography) Pre-coated aluminum sheets kieselgel 60 F254 with fluorescent indicator (MERCK). Melting points (m.p.) were determined on Stuart electrothermal melting point apparatus and were uncorrected. ^{1}H NMR spectra were recorded using a Bruker Advance 400 MHz NMR spectrometer, Faculty of Pharmacy, Beni Suef University; chemical shift (δ) in ppm relative to TMS (δ=0 ppm) as internal standard and DMSO-$d_6$as solvent. Coupling constant (*J*) in Hz and the signal are designed as follows: s, singlet; d, doublet; t, triplet; q, quartet; m, multiplet. ^{13}C NMR spectra were carried out on Bruker Advance 101 MHZ spectrometer, Faculty of Pharmacy, Beni Suef University; chemical shift (δ) in ppm relative to TMS (δ=0 ppm) as internal standard and DMSO-$d_6$as solvent. LC-MS was carried out using an Agilent 6420 triple Quad LC Mass Spectrometer, Faculty of Pharmacy, Minia University. Elemental analyses were recorded on Shimadzu GC/ MS-QP5050A, Regional center for Mycology and Biotechnology, Al-Azhar University.

Compounds **1a-b** [29-30], **2a-b** [31], **3a-b** [31], **4a** [20], **4b** [21], **7a-j** [16, 17] and **8 a-j** [17] were prepared according to the previous reported studies.

4.1.1. General procedure for synthesis of Xanthine-Chalcone hybrids (9-28)

To a stirred solution of **4a-b** (0.9 mmol) and the appropriate acetylated chalcone derivative **8a-j** (0.9 mmol) in acetonitrile, TEA (0.18 mL/mol) was added, the reaction mixture was stirred at room temperature until a precipitate formed. The obtained precipitate was filtrated off and recrystallized from acetonitrile to afford the target compounds **9-28**.

4.1.1.1. 2-((1,3-Dimethyl-2,6-dioxo-2,3,6,7-tetrahydro-*1H*-purin-8-yl)thio)-*N*-(4-((*E*)-cinnamoylphenyl)acetamide (9)

Straw yellow crystals (0.35 g, 83% yield); m.p > 300 ºC; ^{1}H NMR (400 MHz, DMSO-d_6) δ (ppm): 13.63 (1H, s, N7-*H*), 10.73 (1H, s, O=C-N*H*), 8.18 (2H, d, *J* = 8.6 Hz, Ar-*H*), 7.95 (1H, d, *J* = 15.6 Hz, CH=C*H*), 7.87-7.91 (2H, m, Ar-*H*), 7.78 (2H, d, *J* = 8.6 Hz,Ar-*H*), 7.73 (1H, d, *J* = 15.6 Hz, C*H*=CH), 7.47-7.49 (3H, m, Ar-*H*), 4.26 (2H, s, SCH_2), 3.38 (3H, s, N3-CH_3), 3.18 (3H, s, N1-CH_3); ^{13}C NMR (101 MHz, DMSO-d_6) δ (ppm): 187.99, 166.74, 154.56, 151.45, 148.82, 147.83, 143.91, 143.63, 135.22, 133.01, 130.97, 130.44, 129.37, 129.27, 122.41, 118.99, 108.27, 36.96, 30.20, 28.16; Anal. Calcd. For $C_{24}H_{21}N_5O_4S$ (475.13): C, 60.62; H, 4.45; N, 14.73. Found: C, 60.51; H, 4.58; N, 14.63.

4.1.1.2. 2-((1,3-Dimethyl-2,6-dioxo-2,3,6,7-tetrahydro-*1H*-purin-8-yl)thio)-*N*-(4-((*E*)-3-(2-chlorophenyl)acryloyl)phenyl)acetamide (10)

Orange powder (0.37g, 80.6% yield); m.p > 300 ºC; ^{1}H NMR (400 MHz, DMSO-d_6) δ (ppm): 13.48 (1H, s, N7-*H*), 10.73 (1H, s, O=C-N*H*), 8.20-8.23 (3H, m, CH=C*H* + Ar-*H*), 7.93-8.09 (2H, m, Ar-*H*), 7.78 (2H, d, *J* = 8.5 Hz, Ar-*H*), 7.54-7.60 (1H, m, Ar-*H*), 7.43-7.51 (2H, m, Ar-*H* + C*H*=CH), 4.24 (2H, s, SCH_2), 3.39 (3H, s, N3-

C$\underline{H_3}$), 3.22 (3H, s, N1-C$\underline{H_3}$); ^{13}C NMR (101 MHz, DMSO-d_6) δ(ppm): 187.77, 166.79, 154.57, 151.45, 148.79, 147.83,143.85, 138.47, 134.76, 132.82, 132.70, 132.37, 130.60, 130.48, 129.01, 128.15, 125.16, 119.02, 108.30, 36.95, 30.20, 28.18; Anal. Calcd. For $C_{24}H_{20}ClN_5O_4S$ (509.96): C, 56.52; H, 3.95; N, 13.73. Found: C, 56.79; H, 4.11; N, 13.94.

4.1.1.3. 2-((1,3-Dimethyl-2,6-dioxo-2,3,6,7-tetrahydro-1*H*-purin-8-yl)thio)-*N*-(4-*((E)*-3-(4-chlorophenyl)acryloyl)phenyl)acetamide (11)

Pale yellow powder (0.38g, 82% yield); m.p > 300 ºC; ^{1}H NMR (400 MHz, DMSO-d_6) δ (ppm): 13.63 (1H, s, N7-$\underline{H}$), 10.71 (1H, s, O=C-N$\underline{H}$), 8.18 (2H, d, *J* = 8.8 Hz, Ar-$\underline{H}$), 7.97 (1H, d, *J* = 15.6 Hz, CH=C$\underline{H}$), 7.93 (2H, d, *J* = 8.6 Hz, Ar-$\underline{H}$), 7.77 (2H, d, *J* = 8.8 Hz, Ar-$\underline{H}$), 7.71 (1H, d, *J* = 15.6 Hz, C$\underline{H}$=CH),7.53 (2H, d, *J* = 8.6 Hz, Ar-$\underline{H}$), 4.26 (2H, s, SC$\underline{H_2}$), 3.39 (3H, s, N3-C$\underline{H_3}$), 3.22 (3H, s, N1-C$\underline{H_3}$); ^{13}C NMR (101 MHz, DMSO) δ (ppm): 187.86, 166.91, 153.79, 151.39, 148.68, 143.73, 142.42, 135.44, 134.22, 132.91, 130.98, 130.51, 129.40, 123.16, 118.98, 108.32, 99.99, 37.45, 30.20, 28.18; Anal. Calcd. For $C_{24}H_{20}ClN_5O_4S$ (509.96): C, 56.52; H, 3.95; N, 13.73. Found: C, 56.09; H, 4.12; N, 14.01.

4.1.1.4. 2-((1,3-Dimethyl-2,6-dioxo-2,3,6,7-tetrahydro-1*H*-purin-8-yl)thio)-*N*-(4-((*E*)-3-(4-bromophenyl)acryloyl)phenyl)acetamide (12)

White crystal (0.43g, 86% yield); m.p> 300 ºC; ^{1}H NMR (400 MHz, DMSO-d_6) δ (ppm): 13.63 (1H, s, N7-$\underline{H}$), 10.72 (1H, s, O=C-N $\underline{H}$), 8.18 (2H, d, *J* = 8.8 Hz, Ar-$\underline{H}$), 8.00 (1H, d, *J* = 15.7 Hz, CH=C$\underline{H}$), 7.87 (2H, d, *J* = 8.8 Hz, Ar-$\underline{H}$), 7.78 (2H, d, *J* = 8.5 Hz, Ar-$\underline{H}$), 7.76 (1H, d, *J* = 15.7 Hz, C$\underline{H}$=CH),7.68 (2H, d, *J* = 8.5 Hz, Ar-$\underline{H}$), 4.26 (2H, s, SC$\underline{H_2}$), 3.39 (3H, s, N3-C$\underline{H_3}$), 3.22 (3H, s, N1-C$\underline{H_3}$); ^{13}C NMR (101 MHz, DMSO) δ (ppm): 187.89, 166.94, 153.80, 151.40, 148.73, 143.74, 142.52,

134.55, 132.91, 132.34, 131.19, 130.51, 124.32, 123.21, 119.00, 108.33, 99.98, 37.09, 30.19, 28.18; Anal. Calcd. For $C_{24}H_{20}BrN_5O_4S$ (554.42): C, 51.99; H, 3.64; N, 12.63. Found: C, 52.23; H, 3.81; N, 12.89.

4.1.1.5. 2-((1,3-Dimethyl-2,6-dioxo-2,3,6,7-tetrahydro-1*H*-purin-8-yl)thio)-*N*-(4-((*E*)-3-(4-methoxyphenyl)acryloyl)phenyl)acetamide (13)

White powder (0.36 g, 79.5% yield); m.p > 300 ºC; ^{1}H NMR (400 MHz, DMSO-d_6) δ (ppm): 13.63 (1H, s, N7-H), 10.69 (1H, s, O=C-NH), 8.15 (2H, d, *J* = 8.8 Hz,Ar-H), 7.84 (2H, d, *J* = 8.8 Hz, Ar-H), 7.79 – 7.73 (3H, m, CH=CH + Ar-H), 7.70 (1H, d, *J* = 15.5 Hz, CH=CH), 7.02 (2H, d, *J* = 8.8 Hz, Ar-H), 4.26 (2H, s, SCH_2), 3.83 (3H, s, OCH_3), 3.39 (3H, s, N3-CH_3), 3.22 (3H, s, N1-CH_3); ^{13}C NMR (101 MHz, DMSO) δ (ppm): 187.85, 166.85, 161.74, 153.79, 151.38, 148.71, 148.68, 143.88, 143.44, 133.29, 131.15, 130.28, 127.86, 119.86, 118.96, 114.85, 108.32, 55.84, 37.10, 30.20, 28.17; Anal. Calcd. For $C_{25}H_{23}N_5O_5S$ (505.55): C, 59.39; H, 4.59; N, 13.85. Found: C, 59.21; H, 4.80; N, 14.12.

4.1.1.6. 2-((1,3-Dimethyl-2,6-dioxo-2,3,6,7-tetrahydro-1*H*-purin-8-yl)thio)-*N*-(4-((*E*)-3-(3,4-dimethoxyphenyl)acryloyl)phenyl)acetamide (14)

White powder (0.39 g, 81% yield); m.p > 300 ºC; ^{1}H NMR (400 MHz, DMSO-d_6) δ (ppm):13.63 (1H, s, N7-H),10.73 (1H, s, O=C-NH), 8.17 (2H, d, *J* = 8.7 Hz, Ar-H), 7.83 (1H, d, *J* = 15.5 Hz, CH=CH), 7.77 (2H, d, *J* = 8.7 Hz,Ar-H), 7.69 (1H, d, *J* = 15.5 Hz, CH=CH), 7.54 (1H, s,Ar-H), 7.38 (1H, d, *J* = 8.3 Hz, Ar-H), 7.03 (1H, d, *J* = 8.3 Hz, Ar-H), 4.26 (2H, s, SCH_2), 3.87 (3H, s, OCH_3), 3.82 (3H, s, OCH_3), 3.39 (3H, s, N3-CH_3), 3.22 (3H, s, N1-CH_3); ^{13}C NMR (101 MHz, DMSO) δ (ppm): 187.84, 166.89, 153.78, 151.66, 151.39, 149.47, 148.71, 148.63, 144.44, 143.47, 133.29, 130.32, 128.04, 124.35, 119.89, 118.94, 112.00, 111.12, 108.40, 56.21, 56.06, 37.10,

30.21, 28.17; Anal. Calcd. For $C_{26}H_{25}N_5O_6S$ (535.57): C, 58.31; H, 4.70; N, 13.08. Found: C, 58.43; H, 4.63; N, 13.31.

4.1.1.7. 2-((1,3-Dimethyl-2,6-dioxo-2,3,6,7-tetrahydro-1*H*-purin-8-yl)thio)-*N*-(4-((*E*)-3-(3,4,5-trimethoxyphenyl)acryloyl)phenyl)acetamide (15)

White crystals (0.39 g, 81% yield); m.p> 300 ºC; ^{1}H NMR (400 MHz, DMSO-d_6) δ (ppm): 13.63 (1H, s, N7-*H*), 10.72 (1H, s, O=C-N*H*), 8.18 (2H, d, *J* = 8.8 Hz, Ar-*H*), 7.89 (1H, d, *J* = 15.5 Hz, CH=C*H*), 7.78 (2H, d, *J* = 8.8 Hz, Ar-*H*), 7.68 (1H, d, *J* = 15.5 Hz, C*H*=CH), 7.23 (2H, s, Ar-*H*), 4.27 (2H, s, SCH_2), 3.87 (6H, s, 2OCH_3), 3.72 (3H, s, OCH_3), 3.39 (3H, s, N3-CH_3), 3.22 (3H, s, N1-CH_3); ^{13}C NMR (101 MHz, DMSO) δ (ppm): 187.89, 166.89, 153.80, 153.56, 151.39, 148.73, 148.70, 144.42, 143.60, 140.13, 133.11, 130.76, 130.43, 121.52, 118.95, 108.34, 106.95, 60.60, 56.61, 37.10, 30.20, 28.17; Anal. Calcd. For $C_{27}H_{27}N_5O_7S$ (565.60): C, 57.34; H, 4.81; N, 12.38. Found: C, 57.59; H, 4.89; N, 12.54.

4.1.1.8. 2-((1,3-Dimethyl-2,6-dioxo-2,3,6,7-tetrahydro-1*H*-purin-8-yl)thio)-*N*-(4-((*E*)-3-(3-nitrophenyl)acryloyl)phenyl)acetamide (16)

Yellowish white powder (0.41g, 87% yield); m.p> 300 ºC; ^{1}H NMR (400 MHz, DMSO-d_6) δ (ppm): 13.63 (1H, s, N7-*H*), 10.74 (1H, s, O=C-N*H*), 8.78 (1H, s, Ar-*H*), 8.34 (1H, d, *J* = 7.8 Hz, Ar-*H*), 8.29 – 8.25 (1H, m, Ar-*H*), 8.23 (2H, d, *J* = 8.8 Hz, Ar-*H*), 8.17 (1H, d, *J* = 15.7 Hz, CH=C*H*), 7.84 (1H, d, *J* = 15.7 Hz, C*H*=CH), 7.80 – 7.72 (3H, m, Ar-*H*), 4.26 (2H, s, SCH_2), 3.39 (3H, s, N3-CH_3), 3.22 (3H, s, N1-CH_3); ^{13}C NMR (101 MHz, DMSO) δ (ppm): 187.82, 166.95, 153.80, 151.38, 148.90, 148.72, 148.69, 143.90, 141.36, 137.15, 135.55, 132.70, 130.81, 130.69, 125.18, 125.03, 123.37, 119.03, 108.35, 37.10, 30.20, 28.17; Anal. Calcd. For $C_{24}H_{20}N_6O_6S$ (520.52): C, 55.38; H, 3.87; N, 16.15. Found: C, 55.57; H, 4.01; N, 16.42.

4.1.1.9. 2-((1,3-Dimethyl-2,6-dioxo-2,3,6,7-tetrahydro-1*H*-purin-8-yl)thio)-*N*-(4-((*E*)-3-(p-tolyl)acryloyl)phenyl)acetamide (17)

Straw yellow powder (0.38 g, 85.5% yield); m.p> 300 ºC; ^{1}H NMR (400 MHz, DMSO-d_6) δ (ppm): 13.63 (1H, s, N7-H), 10.72 (1H, s, O=C-NH), 8.16 (2H, d, *J* = 8.7 Hz, Ar-H), 7.89 (1H, d, *J* = 15.6 Hz, CH=CH), 7.77 (4H, dd, *J* = 8.0, 8.0 Hz, Ar-H), 7.70 (1H, d, *J* = 15.6 Hz, CH=CH), 7.28 (2H, d, *J*= 8.7 Hz, Ar-H), 4.24 (2H, s, SCH_2), 3.39 (3H, s, N3-CH_3), 3.22 (3H, s, N1-CH_3), 2.36 (3H, s, CH_3); ^{13}C NMR (101 MHz, DMSO) δ (ppm): 187.95, 166.89, 153.82, 151.39, 148.71, 148.70, 143.97, 143.57, 141.03, 133.12, 132.51, 130.37, 129.99, 129.31, 121.33, 118.98, 108.35, 37.09, 30.20, 28.17, 21.56; Anal. Calcd. For $C_{25}H_{23}N_5O_4S$ (489.55): C, 61.34; H, 4.74; N, 14.31. Found: C, 61.58; H, 4.90; N, 14.52.

4.1.1.10. 2-((1,3-Dimethyl-2,6-dioxo-2,3,6,7-tetrahydro-1*H*-purin-8-yl)thio)-*N*-(4-((*E*)-3-(2,4-dimethylphenyl)acryloyl)phenyl)acetamide (18)

Straw yellow crystals (0.35g, 78% yield); m.p> 300 ºC; ^{1}H NMR (400 MHz, DMSO-d_6) δ (ppm): 13.63 (1H, s, N7-H), 10.71 (1H, s, O=C-NH), 8.16 (2H, d, *J* = 8.8 Hz, Ar-H), 7.95 (1H, d, *J* = 15.4 Hz, CH=CH), 7.90 (1H, d, *J* = 8.5 Hz, Ar-H), 7.82 – 7.73 (3H, m, Ar-H + CH=CH), 7.10 (2H, d, *J* = 5.2 Hz, Ar-H), 4.26 (2H, s, SCH_2), 3.39 (3H, s, N3-CH_3), 3.22 (3H, s, N1-CH_3), 2.41 (3H, s, CH_3), 2.31 (3H, s, CH_3); ^{13}C NMR (101 MHz, DMSO) δ (ppm): 187.97, 166.88, 153.80, 151.38, 148.71, 143.56, 140.92, 140.68, 138.40, 133.13, 131.90, 130.99, 130.37, 127.55, 127.28, 122.09, 118.99, 108.34, 99.98, 37.09, 30.20, 28.17, 21.41, 19.73; Anal. Calcd. For$C_{26}H_{25}N_5O_4S$ (503.57): C, 62.01; H, 5.00; N, 13.91. Found: C, 61.89; H, 4.88; N, 14.17.

4.1.1.11. 2-((1-Methyl-2,6-dioxo-2,3,6,7-tetrahydro-*1H*-purin-8-yl)thio)-*N*-(4-((*E*)-cinnamoylphenyl)acetamide (19)

Greenish white crystals (0.36 g, 86% yield); m.p> 300 ºC; ^{1}H NMR (400 MHz, DMSO-d_6) δ(ppm): 13.49 (1H, s, N7-*H*), 11.89 (1H, s, N3-*H*),10.71 (1H, s, O=C-N*H*), 8.19 (2H, d, *J* = 8.6 Hz, Ar-*H*), 7.97 (1H, d, *J* = 15.6 Hz, CH=C*H*), 7.87-7.91 (2H, m, Ar-*H*), 7.78 (2H, d, *J* = 8.6 Hz, Ar-*H*), 7.75 (1H, d, *J* = 15.6 Hz, C*H*=CH), 7.46-7.49 (3H, m, Ar-*H*), 4.24 (2H, s, SCH_2), 3.18 (3H, s, N1-CH_3); ^{13}C NMR (101 MHz, DMSO-d_6) δ (ppm): 187.99, 166.74, 154.56, 151.45, 148.82, 147.83, 143.91, 143.63, 135.22, 133.01, 130.97, 130.44, 129.37, 129.27, 122.41, 118.99, 108.27, 36.96, 27.43; Anal. Calcd. For $C_{23}H_{19}N_5O_4S$ (461.49): C, 59.86; H, 4.15; N, 15.18. Found: C, 60.08; H, 4.39; N, 15.42.

4.1.1.12. 2-((1-Methyl-2,6-dioxo-2,3,6,7-tetrahydro-*1H*-purin-8-yl)thio)-*N*-(4-((*E*)-3-(2-chlorophenyl)acryloyl)phenyl)acetamide (20)

Pale yellow powder (0.37 g, 80.6% yield); m.p> 300 ºC; ^{1}H NMR (400 MHz, DMSO-d_6) δ (ppm):13.48 (1H, s, N7-*H*), 11.89 (1H, s, N3-*H*), 10.73 (1H, s, O=C-N*H*), 8.20-8.00 (3H, m, CH=C*H* + Ar-*H*), 7.93-8.09 (2H, m, Ar-*H*), 7.78 (2H, d, *J* = 8.5 Hz, Ar-*H*),7.54-7.60 (1H, m, Ar-*H*), 7.43-7.51 (2H, m, Ar-*H* + C*H*=CH), 4.24 (2H, s, SCH_2), 3.18 (3H, s, N1-CH_3); ^{13}C NMR (101 MHz, DMSO-d_6) δ (ppm): 187.77, 166.79, 154.57, 151.45, 148.79, 147.83, 143.85, 138.47, 134.76, 132.82, 132.70, 132.37, 130.60, 130.48, 129.01, 128.15, 125.16, 119.02, 108.30, 36.95, 27.43; Anal. Calcd. For $C_{23}H_{18}ClN_5O_4S$ (495.94): C, 55.70; H, 3.66; N, 14.12. Found: C, 55.59; H, 3.87; N, 14.40.

4.1.1.13. 2-((1-Methyl-2,6-dioxo-2,3,6,7-tetrahydro-1*H*-purin-8-yl)thio)-*N*-(4-*((E)*-3-(4-chlorophenyl)acryloyl)phenyl)acetamide (21)

Olive green powder (0.36 g, 81% yield); m.p> 300 ºC; ^{1}H NMR (400 MHz, DMSO-d_6) δ (ppm): 13.63 (1H, s, N7-H), 11.89 (1H, s, N3-H), 10.71 (1H, s, O=C-NH), 8.18 (2H, d, *J* = 8.8 Hz, Ar-H), 7.99 (1H, d, *J* = 15.6 Hz, CH=CH), 7.95 (2H, d, *J* = 8.6 Hz, Ar-H), 7.79 (2H, d, *J* = 8.8 Hz, Ar-H), 7.73 (1H, d, *J* = 15.6 Hz, CH=CH), 7.54 (2H, d, *J* = 8.6 Hz, Ar-H), 4.24 (2H, s, SCH_2), 3.18 (3H, s, N1-CH_3); ^{13}C NMR (101 MHz, DMSO) δ (ppm): 187.88, 166.76, 154.59, 151.45, 148.82, 147.83, 143.70, 142.43, 135.44, 134.20, 132.90, 131.03, 130.49, 129.40, 123.15, 118.99, 108.30, 36.94, 27.43; Anal. Calcd. For $C_{23}H_{18}ClN_5O_4S$ (495.94): C, 55.70; H, 3.66; N, 14.12. Found: C, 55.92; H, 3.75; N, 14.38.

4.1.1.14. 2-((1-Methyl-2,6-dioxo-2,3,6,7-tetrahydro-1*H*-purin-8-yl)thio)-*N*-(4-((*E*)-3-(4-bromophenyl)acryloyl)phenyl)acetamide (22)

White powder (0.40 g, 83% yield); m.p> 300 ºC; ^{1}H NMR (400 MHz, DMSO-d_6) δ (ppm): 13.47 (1H, s, N7-H), 11.89 (1H, s, N3-H), 10.73 (1H, s, O=C-NH), 8.19 (2H, d, *J* = 8.8 Hz, Ar-H), 8.00 (1H, d, *J* = 15.7 Hz, CH=CH), 7.87 (2H, d, *J* = 8.6 Hz, Ar-H), 7.78 (2H, d, *J* = 8.8 Hz, Ar-H), 7.72 (1H, d, *J* = 15.7 Hz, CH=CH), 7.68 (2H, d, *J* = 8.6 Hz, Ar-H), 4.23 (2H, s, SCH_2), 3.18 (3H, s, N1-CH_3); ^{13}C NMR (101 MHz, DMSO) δ (ppm): 187.87, 166.76, 154.59, 151.45, 147.88, 143.72, 142.52, 134.55, 132.89, 132.33, 131.20, 130.50, 124.31, 123.21, 118.98, 108.28, 99.98, 36.96, 27.43; Anal. Calcd. For $C_{23}H_{18}BrN_5O_4S$ (540.39): C, 51.12; H, 3.36; N, 12.96. Found: C, 51.36; H, 3.08; N, 13.19.

4.1.1.15. 2-((1-Methyl-2,6-dioxo-2,3,6,7-tetrahydro-1*H*-purin-8-yl)thio)-*N*-(4-((*E*)-3-(4-methoxyphenyl)acryloyl)phenyl)acetamide (23)

White crystal (0.36 g, 82% yield); m.p> 300 ºC; ^{1}H NMR (400 MHz, DMSO-d_6) δ (ppm): 13.48 (1H, s, N7-*H*), 11.89 (1H, s, N3-*H*), 10.69 (1H, s, O=C-N*H*), 8.15 (2H, d, *J* = 8.6 Hz, Ar-*H*), 7.84 (2H, d, *J* = 8.8 Hz, Ar-*H*), 7.79–7.74 (3H, m, CH=C*H* + Ar-*H*), 7.70 (1H, d, *J* = 15.5 Hz, C*H*=CH), 7.03 (2H, d, *J* = 8.8 Hz, Ar-*H*), 4.23 (2H, s, SCH_2), 3.83 (3H, s, OCH_3), 3.18 (3H, s, N1-CH_3); ^{13}C NMR (101 MHz, DMSO) δ (ppm): 187.87, 166.70, 161.75, 154.56, 151.45, 148.84, 147.83, 143.92, 143.42, 133.29, 131.17, 130.28, 127.86, 119.87, 118.97, 114.87, 108.25, 55.85, 36.94, 27.43; Anal. Calcd. For $C_{24}H_{21}N_5O_5S$ (491.52): C, 58.65; H, 4.31; N, 14.25. Found: C, 58.87; H, 4.49; N, 14.43.

4.1.1.16. 2-((1-Methyl-2,6-dioxo-2,3,6,7-tetrahydro-1*H*-purin-8-yl)thio)-*N*-(4-((*E*)-3-(3,4-dimethoxyphenyl)acryloyl)phenyl)acetamide (24)

White powder (0.41g, 87% yield); m.p> 300 ºC; ^{1}H NMR (400 MHz, DMSO-d_6) δ(ppm): 13.48 (1H, s, N7-*H*), 11.89 (1H, s, N3-*H*), 10.70 (1H, s, O=C-N*H*), 8.17 (2H, d, *J* = 8.7 Hz, Ar-*H*), 7.83 (1H, d, *J* = 15.5 Hz, CH=C*H*), 7.77 (2H, d, *J* = 8.7 Hz, Ar-*H*), 7.69 (1H, d, *J* = 15.5 Hz, C*H*=CH), 7.54 (1H, s, Ar-*H*), 7.38 (1H, d, *J* = 8.3 Hz, Ar-*H*), 7.03 (1H, d, *J* = 8.4 Hz, Ar-*H*), 4.24 (2H, s, SCH_2), 3.87 (3H, s, OCH_3), 3.82 (3H, s, OCH_3), 3.18 (3H, s, N1-CH_3); ^{13}C NMR (101 MHz, DMSO) δ (ppm): 187.85, 166.71, 154.56, 151.67, 151.45, 149.48, 148.84, 147.83, 144.45, 143.44, 133.29, 130.31, 128.05, 124.36, 119.90, 118.94, 112.02, 111.14, 108.27, 56.22, 56.07, 36.95, 27.43; Anal. Calcd. For $C_{25}H_{23}N_5O_6S$ (521.55): C, 57.57; H, 4.44; N, 13.43. Found: C, 57.80; H, 4.58; N, 13.70.

4.1.1.17. 2-((1-Methyl-2,6-dioxo-2,3,6,7-tetrahydro-1*H*-purin-8-yl)thio)-*N*-(4-((*E*)-3-(3,4,5-trimethoxyphenyl)acryloyl)phenyl)acetamide (25)

White crystals (0.42g, 85% yield); m.p> 300 ºC; ^{1}H NMR (400 MHz, DMSO-d_6) δ (ppm): 13.48 (1H, s, N7-*H*), 11.89 (1H, s, N3-*H*), 10.71 (1H, s, O=C-N*H*), 8.18 (2H, d, *J* = 8.8 Hz, Ar-*H*), 7.89 (1H, d, *J* = 15.5 Hz, CH=C*H*), 7.78 (2H, d, *J* = 8.8 Hz, Ar-*H*), 7.68 (1H, d, *J* = 15.5 Hz, C*H*=CH), 7.23 (2H, s, Ar-*H*), 4.24 (2H, s, SCH_2), 3.87 (6H, s, 2OCH_3), 3.72 (3H, s, OCH_3), 3.18 (3H, s, N1-CH_3); ^{13}C NMR (101 MHz, DMSO) δ (ppm): 187.89, 166.72, 154.55, 153.56, 151.45, 148.82, 147.83, 144.43, 143.57, 140.14, 133.11, 130.77, 130.42, 121.53, 118.95, 108.26, 106.95, 60.60, 56.61, 36.96, 27.43; Anal. Calcd. For $C_{26}H_{25}N_5O_7S$ (551.57): C, 56.62; H, 4.57; N, 12.70. Found: C, 56.86; H, 4.73; N, 12.97.

4.1.1.18. 2-((1-Methyl-2,6-dioxo-2,3,6,7-tetrahydro-1*H*-purin-8-yl)thio)-*N*-(4-((*E*)-3-(3-nitrophenyl)acryloyl)phenyl)acetamide (26)

Pale brown powder (0.36g, 78% yield); m.p> 300 ºC; ^{1}H NMR (400 MHz, DMSO-d_6) δ (ppm): 13.48 (1H, s, N7-*H*), 11.89 (1H, s, N3-*H*), 10.73 (1H, s, O=C-N*H*), 8.78 (1H, s, Ar-*H*), 8.33 (1H, d, *J* = 7.8 Hz, Ar-*H*), 8.30 – 8.25 (1H, m, Ar-*H*), 8.24 (2H, d, *J* = 8.8 Hz, Ar-*H*), 8.17 (1H, d, *J* = 15.7 Hz, CH=C*H*), 7.84 (1H, d, *J* = 15.7 Hz, C*H*=CH), 7.80–7.72 (3H, m, Ar-*H*), 4.24 (2H, s, SCH_2), 3.18 (3H, s, N1-CH_3); ^{13}C NMR (101 MHz, DMSO) δ (ppm): 187.83, 166.79, 154.56, 151.45, 148.89, 148.82, 147.83, 143.87, 141.37, 137.14, 135.54, 132.70, 130.81, 130.68, 125.17, 125.04, 123.38, 118.99, 108.27, 36.95, 27.43; Anal. Calcd. For $C_{23}H_{18}N_6O_6S$ (506.49): C, 54.54; H, 3.58; N, 16.59. Found: C, 54.78; H, 3.49; N, 16.75.

4.1.1.19. 2-((1-Methyl-2,6-dioxo-2,3,6,7-tetrahydro-1*H*-purin-8-yl)thio)-*N*-(4-((*E*)-3-(p-tolyl)acryloyl)phenyl)acetamide (27)

Pale yellow powder (0.33g, 78% yield); m.p> 300 ºC; ^{1}H NMR (400 MHz, DMSO-d_6) δ (ppm): 13.48 (1H, s, N7-*H*), 11.89 (1H, s, N3-*H*), 10.70 (1H, s, O=C-N*H*), 8.16 (2H, d, *J* = 8.7 Hz, Ar-*H*), 7.89 (1H, d, *J* = 15.6 Hz, CH=C*H*), 7.77 (4H, dd, *J* = 8.1, 8.1 Hz, Ar-*H*), 7.70 (1H, d, *J* = 15.6 Hz, C*H*=CH), 7.28 (2H, d, *J*= 8.7 Hz, Ar-*H*), 4.24 (2H, s, SCH_2), 3.18 (3H, s, N1-CH_3), 2.36 (3H, s, CH_3); ^{13}C NMR (101 MHz, DMSO) δ (ppm): 187.94, 166.71, 154.55, 151.45, 148.82, 147.83, 143.98, 143.55, 141.04, 133.12, 132.51, 130.37, 130.00, 129.32, 121.33, 118.98, 108.25, 36.95, 27.43, 21.56; Anal. Calcd. For $C_{24}H_{21}N_5O_4S$ (475.52): C, 60.62; H, 4.45; N, 14.73. Found: C, 60.49; H, 4.62; N, 14.95.

4.1.1.20. 2-((1-Methyl-2,6-dioxo-2,3,6,7-tetrahydro-1*H*-purin-8-yl)thio)-*N*-(4-((*E*)-3-(2,4-dimethylphenyl)acryloyl)phenyl)acetamide (28)

Straw yellow crystals(0.37g, 83.5% yield); m.p> 300 ºC; ^{1}H NMR (400 MHz, DMSO-d_6) δ (ppm):13.47 (1H, s, N7-*H*),11.89 (1H, s, N3-*H*), 10.71 (1H, s, O=C-N*H*), 8.16 (2H, d, *J* = 8.8 Hz, Ar-*H*), 7.90 (1H, d, *J* = 15.4 Hz, CH=C*H*), 7.90 (1H, d, *J* = 8.5 Hz, Ar-*H*), 7.82–7.74 (3H, m, Ar-*H* + C*H*=CH), 7.11 (2H, d, *J* = 5.2 Hz, Ar-*H*), 4.23 (2H, s, SCH_2), 3.18 (3H, s, N1-CH_3), 2.41 (3H, s, CH_3), 2.31 (3H, s, CH_3); ^{13}C NMR (101 MHz, DMSO) δ (ppm): 187.97, 166.72, 154.59, 151.45, 148.81, 143.54, 140.94, 140.69, 138.41, 133.13, 131.91, 130.99, 130.37, 127.56, 127.29, 122.09, 118.99, 108.29, 99.98, 36.96, 27.43, 21.41, 19.74; Anal. Calcd. For $C_{25}H_{23}N_5O_4S$ (489.55): C, 61.34; H, 4.74; N, 14.31. Found: C, 61.62; H, 4.87; N, 14.59.

4.2. Biological evaluation

4.2.1. Cytotoxic activity using MTT Assay and evaluation of IC_{50}

4.2.1.1. MTT assay

MTT assay was performed to investigate the effect of the synthesized compounds on mammary epithelial cells (MCF-10A) [32]. **See Appendix A**.

4.2.1.2. Assay for antiproliferative effect

To explore the antiproliferative potential of compounds MTT assay was performed [32] using different cell lines. **See Appendix A**.

4.2.2. EGFR inhibitory assay

A cell-free assay was used to explore the mechanism of inhibition of EGFR kinase of the most active compounds according to the reported method [33]. **See Appendix A**.

4.2.3. Caspase-3 and 8 activation assay

Cell line cells of MCF-7 and HepG2 were obtained from ATCC. RPMI 1640 containing 10% FBS was used to allow cells to grow at 37 ^{o}C, stimulated with the compounds to be tested for caspase-3 or caspase-8 [34]. **See Appendix A**.

4.2.4. Evaluation of Bax and Bcl-2 expressions

m RNA isolation was carried out using RNeasy extraction kit, up to 1 X 10^7 cells. They were disrupted in Buffer RLT and homogenized [35] **See Appendix A**.

4.2.5. Cell apoptosis assay

Apoptosis was determined by flow cytometry based on the Annexin-V-fluoresce in isothiocyanate (FITC) and propidium iodide (PI) stainingkit (BD Pharmingen, San Diego, USA) [36]. **See Appendix A**.

4.3. Docking study

The 3.5 Å3D structureof EGFR (PDB ID: 1M17) in complex with AQ4999 was downloaded from protein data bank [37]. All molecular modeling calculations and docking studies were carried out using Discovery Studio software 2016 client v16.1.0.15350 (San Diego, CA) with CDOCKER program. **See Appendix A.**

5. Conclusion

In the present study, 20 new final compounds **(9-28)** assembly two bioactive entities chalcone and xanthine derivative in only one solid hybrid structure were synthesized, characterized and evaluated for their anti-proliferative activity *in vitro* on selected human cancer cell lines. Compounds **10**, **11**, **13**, **14**, **16**, **20** and **23** exhibited potent inhibition of cancer cells growth compared to doxorubicin as a reference. Compounds **10**, **11**, **13**, **14**, **16**, **20** and **23** were evaluated for their EGFR inhibitory effect. Compound **11** showed IC_{50} = 0.3 µM on the target enzyme which is more potent than staurosporine reference (IC_{50} = 0.4 µM). Accordingly, the apoptotic effect of compounds **11** was extensively investigated and showed a marked increase in Bax level and down-regulation in Bcl2 in comparison to the control. Furthermore, the effect of compound **11** on Caspases 3 and 8 was evaluated and was found to increase their levels by 8 and 14 folds, respectively. Also, the effect of compound **11** on the cell cycle and its cytotoxic effect were examined. Moreover, a molecular docking study was adopted to explain and confirm the mechanism of action. These results led to discovery of novel promising xanthine-chalcone hybrids with high potency against cancer cell lines that warranted further investigation and development as potential anti-cancer candidates.

References

[1] L.A. Torre, F. Bray, R.L. Siegel, J. Ferlay, J. Lortet-Tieulent, A. Jemal, Global cancer statistics, CA. 65 (2015) 87-108.

[2] K.D. Miller, R.L. Siegel, C.C. Lin, A.B. Mariotto, J.L. Kramer, J.H. Rowland, K.D. Stein, R. Alteri, A. Jemal, Cancer treatment and survivorship statistics, CA. 66 (2016) 271-289.

[3] B.A. Chabner, T.G. Roberts Jr, Chemotherapy and the war on cancer, Nat. Rev. Cancer 5 (2005) 65.

[4] A. Coolbrandt, K. Van den Heede, E. Vanhove, A. De Bom, K. Milisen, H. Wildiers, Immediate versus delayed self-reporting of symptoms and side effects during chemotherapy: does timing matter?, Eur. J. Oncol. Nurs. 15 (2011) 130-136.

[5] M.S. Abdelbaset, G.E.-D.A. Abuo-Rahma, M.H. Abdelrahman, M. Ramadan, B.G. Youssif, S.N.A. Bukhari, M.F. Mohamed, M. Abdel-Aziz, Novel Pyrrol-2 (3H)-ones and Pyridazin-3 (2H)-ones Carrying Quinoline Scaffold as Anti-proliferative Tubulin Polymerization Inhibitors, Bioorg. Chem. 80 (2018) 151-163.

[6] H.L. Qin, J. Leng, B.G. Youssif, M.W. Amjad, M.A.G. Raja, M.A. Hussain, Z. Hussain, S.N. Kazmi, S.N.A. Bukhari, Synthesis and mechanistic studies of curcumin analog-based oximes as potential anticancer agents, Chem. Biol. Drug Des. 90 (2017) 443-449.

[7] T. Motegi, M. Katayama, Y. Uzuka, Y. Okamura, Evaluation of anticancer effects and enhanced doxorubicin cytotoxicity of xanthine derivatives using canine hemangiosarcoma cell lines, Res. Vet. Sci. 95 (2013) 600-605.

[8] L. Hirsh, A. Dantes, B.-S. Suh, Y. Yoshida, K. Hosokawa, K. Tajima, F. Kotsuji, O. Merimsky, A. Amsterdam, Phosphodiesterase inhibitors as anti-cancer drugs, Biochem Pharmacol. 68 (2004) 981-988.

[9] Y. Voynikov, G. Momekov, P. Peikov, G. Stavrakov, Cytotoxicity assay on several theophylline-7-acetic acid amides with amino acids, Pharmacia 61 (2014) 12-16.

[10] C.H. Misirlioglu, T. Demirkasimoglu, B. Kucukplakci, E. Sanri, K. Altundag, Pentoxifylline and alpha-tocopherol in prevention of radiation-induced lung toxicity in patients with lung cancer, Med. Oncol. 24 (2007) 308-311.

[11] A. Bravo-Cuellar, G. Hernández-Flores, J.M. Lerma-Díaz, J.R. Domínguez-Rodríguez, L.F. Jave-Suárez, R. De Célis-Carrillo, A. Aguilar-Lemarroy, P. Gómez-Lomeli, P.C. Ortiz-Lazareno, Pentoxifylline and the proteasome inhibitor MG132 induce apoptosis in human leukemia U937 cells through a decrease in the expression of Bcl-2 and Bcl-XL and phosphorylation of p65, J. Biomed. Sci. 20 (2013) 13.

[12] P.N. Goel, R.P. Gude, Pentoxifylline regulates the cellular adhesion and its allied receptors to extracellular matrix components in breast cancer cells, Biomed. Pharmacother. 68 (2014) 93-99.

[13] F.F. Ahmed, A.A.A. El-Hafeez, S.H. Abbas, D. Abdelhamid, M. Abdel-Aziz, New 1, 2, 4-triazole-Chalcone hybrids induce Caspase-3 dependent apoptosis in A549 human lung adenocarcinoma cells, Eur. J. Med. Chem. 151 (2018) 705-722.

[14] P. Singh, A. Anand, V. Kumar, Recent developments in biological activities of chalcones: A mini review, Eur. J. Med. Chem. 85 (2014) 758-777.

[15] S. Park, E.H. Kim, J. Kim, S.H. Kim, I. Kim, Biological evaluation of indolizine-chalcone hybrids as new anticancer agents, Eur. J. Med. Chem. 144 (2018) 435-443.

[16] M.A. Mourad, M. Abdel-Aziz, G.E.-D.A. Abuo-Rahma, H.H. Farag, Design, synthesis and anticancer activity of nitric oxide donating/chalcone hybrids, Eur. J. Med. Chem. 54 (2012) 907-913.

[17] M. Abdel-Aziz, S.-E. Park, G.E.-D.A. Abuo-Rahma, M.A. Sayed, Y. Kwon, Novel N-4-piperazinyl-ciprofloxacin-chalcone hybrids: synthesis, physicochemical properties, anticancer and topoisomerase I and II inhibitory activity, Eur. J. Med. Chem. 69 (2013) 427-438.

[18] A.M. Hayallah, M. Famulok, Synthesis of new 1, 3, 8-trisubstituted purine-2, 6-diones and 1, 3, 6-trisubstituted thiazolo [2, 3-f] purine-2, 4-diones, J. Heterocycl. Chem. 74 (2007) 369-382.

[19] C.E. Müller, J. Sandoval-Ramírez, A new versatile synthesis of xanthines with variable substituents in the 1-, 3-, 7-and 8-positions, Synthesis 1995 (1995) 1295-1299.

[20] W.A. Elgaher, A.M. Hayallah, O.I. Salem, A. Abdel Alim, Synthesis, anti-bronchoconstrictive, and antibacterial activities of some new 8-substituted-1, 3-dimethylxanthine derivatives, Bull. Pharm. Sci., Assiut University 32 (2009) 153-187.

[21] A. Hayallah, Design and synthesis of new 1, 8-disubstituted purine-2, 6-diones and 3, 6-disubstituted thiazolo [2, 3-f] purine-2, 4-diones as potential antinociceptive and antiinflammatory agents, Pharmacia 54 (2007) 3-13.

[22] O.F. Abou-Ghadir, A.M. Hayallah, S.G. Abdel-Moty, M.A. Hussein, Design and synthesis of some new purine-dione derivatives of potential anti-inflammatory activity, Der pharma chem. 6 (2014) 199-211.

[23] G.E.-D.A. Abuo-Rahma, M. Abdel-Aziz, M.A. Mourad, H.H. Farag, Synthesis, anti-inflammatory activity and ulcerogenic liability of novel nitric oxide donating/chalcone hybrids, Bioorganic Med. Chem. 20 (2012) 195-206.

[24] S. Nagata, Apoptosis mediated by Fas and its related diseases, Nihon Ika Daigaku Zasshi. 64 (1997) 459.

[25] S. Cory, J.M. Adams, The Bcl2 family: regulators of the cellular life-or-death switch, Nat. Rev. Cancer 2 (2002) 647-656.

[26] A.J. Giaccia, M.B. Kastan, The complexity of p53 modulation: emerging patterns from divergent signals, Genes Dev. 12 (1998) 2973-2983.

[27] D. Lietha, M.J. Eck, Crystal structures of the FAK kinase in complex with TAE226 and related bis-anilino pyrimidine inhibitors reveal a helical DFG conformation, PloS One. 3 (2008) 3800.

[28] J. Stamos, M.X. Sliwkowski, C. Eigenbrot, Structure of the epidermal growth factor receptor kinase domain alone and in complex with a 4-anilinoquinazoline inhibitor, J. Biol. Chem. 277 (2002) 46265-46272.

[29] V. Papesch, E.F. Schroeder, Synthesis of 1-mono-and 1, 3-di-substituted 6-aminouracils. Diuretic activity, J. Org. Chem. 16 (1951) 1879-1890.

[30] C.E. Müller, Synthesis of 3-substituted 6-aminouracils, Tetrahedron letters 32 (1991) 6539-6540.

[31] C.E. Müller, General synthesis and properties of 1-monosubstituted xanthines, Synthesis. (1993) 125-128.

[32] B. G.M. Youssif, M. H. Abdelrahman, A.H. Abdelazeem, M. A. abdelgawad, H. M. Ibrahim, O.I.A. Salem, M.F.A. Mohamed, L. Treambleau, S.N. A. Bukhari,

Design, synthesis, mechanistic and histopathological studies of small molecules of novel indole-2-carboxamides and pyrazino[1,2-a]indol-1(2H)-ones as potential anticancer agents effecting the reactive oxygen species production, Eur. J. Med. Chem. 146 (2018) 260-273.

[33] F. Manetti, G.A. Locatelli, G. Maga, S. Schenone, M. Modugno, S. Forli, F. Corelli, M. Botta, A Combination of Docking/Dynamics Simulations and Pharmacophoric Modeling To Discover New Dual c-Src/Abl Kinase Inhibitors, J. Med. Chem. 49 (2006) 3278-3286.

[34] J. Wang, M. J. Lenardo, Roles of caspases in apoptosis, development, and cytokine maturation revealed by homozygous gene deficiencies, J. Cell Sci. 113 (2000) 753-757.

[35] T. Mitupatum, K. Aree, S. Kittisenachai, S. Roytrakul, S. Puthong, S. Kangsadalampai, P. Rojpibulstit, mRNA Expression of Bax, Bcl-2, p53, Cathepsin B, Caspase-3 and Caspase-9 in the HepG2 Cell Line Following Induction by a Novel Monoclonal Ab Hep88 mAb: Cross-Talk for Paraptosis and Apoptosis, Asian Pac J Cancer Prev. 17 (2016) 703-712.

[36] H. A. M. El-Sherief, B. G. M. Youssif, S. N. A. Bukhari, A. H. Abdelazeem, M. Abdel-Aziz, H. M. Abdel-Rahman, Synthesis, anticancer activity and molecular modeling studies of 1,2,4-triazole derivatives as EGFR inhibitors, Eur. J. Med. Chem. 156 (2018) 774-789

[37] R.B. Ravelli, B. Gigant, P.A. Curmi, I. Jourdain, S. Lachkar, A. Sobel, M. Knossow, Insight into tubulin regulation from a complex with colchicine and a stathmin-like domain, Nature 428 (2004) 198.